Electronic Supplementary Material (ESI) for Journal of Materials Chemistry A.
This journal is © The Royal Society of Chemistry 2017

# Facile and tailored synthesis of ultrahigh-surface-area clews of carbon nanobelts for high-rate lithium-sulfur batteries

Shao-Zhong Zeng [a,b], Xierong Zeng [a,b], Wenxuan Tu [a], Yuechao Yao [a], Liang Yu [a], Hongliang Wu [a], Wenwu Jin [a], Haitao Huang [c], and Jizhao Zou [a,*]

[a] Shenzhen Key Laboratory of Special Functional Materials & Shenzhen Engineering Laboratory for Advance Technology of Ceramics, College of Materials Science and Engineering, Shenzhen University, Shenzhen 518060, PR China. Email: zoujizhao@szu.edu.cn.

[b] Key Laboratory of Optoelectronic Devices and Systems of Ministry of Education and Guangdong Province, College of Optoelectronic Engineering, Shenzhen University, Shenzhen 518060, P. R. China.

[c] Department of Applied Physics, The Hong Kong Polytechnic University, Hung Hom, Kowloon, Hong Kong, P. R. China.

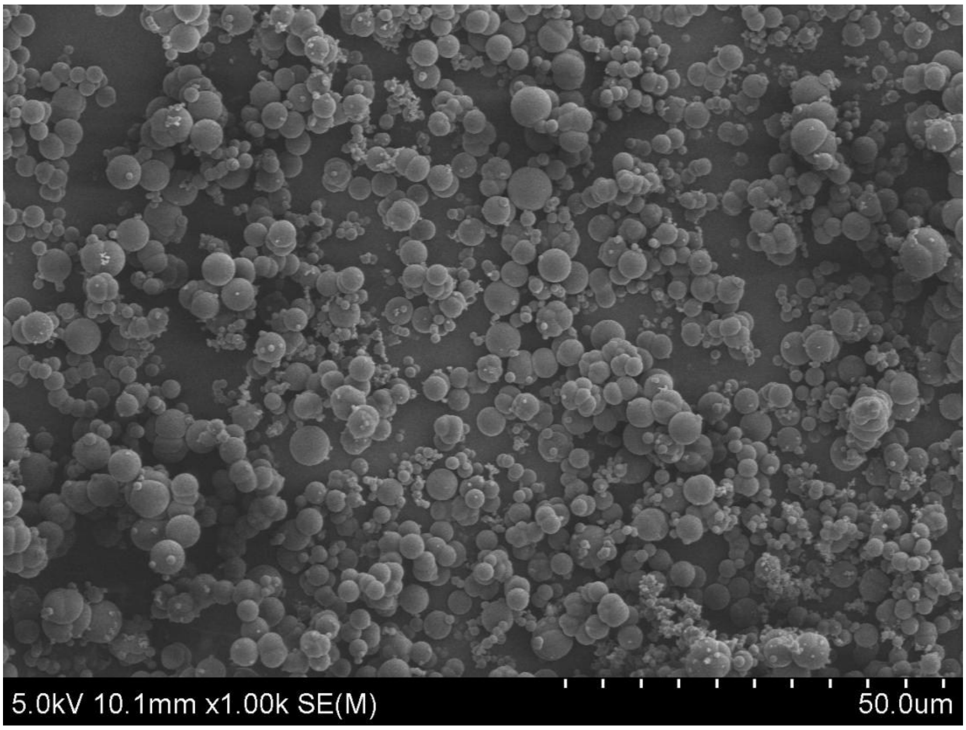

Figure S1. SEM image of the products formed by the reaction between catechol and formaldehyde

Table S1. BET surface area, pore volume and synthesis process of some typical HPCs.

| Number | $S_{BET}$ ( $m^2\ g^{-1}$) | Pore volume ($cm^3\ g^{-1}$) | Synthesis process | References |
|---|---|---|---|---|
| 1 | 2157 | 2.26 | Pig bone, KOH activation | [1] |
| 2 | 2300 | 2.0 | Phenolic resin, F127 template. | [2] |
| 3 | 1750 | 1.57 | Agar, KOH activation | [3] |
| 4 | 2494 | 2.28 | Silk, ZnCl2 and FeCl3 as templates and activators | [4] |
| 5 | 2870 | 2.19 | PPy microsheets, KOH activation | [5] |
| 6 | 1276 | 4.18 | mesoporous metal oxide flakes as templates, CVD | [6] |
| 7 | 2449 | 4.97 | Silica nanospheres as templates to prepare silicon carbide which is further converted into porous carbon by chlorination | [7] |
| 8 | 3060 | 3.45 | ZnO nanoparticals as templates and activators, | [8] |
| 9 | 2749 | 2.09 | Mesoporous silica (SBA-15) as a template, $CO_2$ activation. | [9] |
| 10 | 3445 | 3.18 | Direct carbonization and $CO_2$ activation | This work |

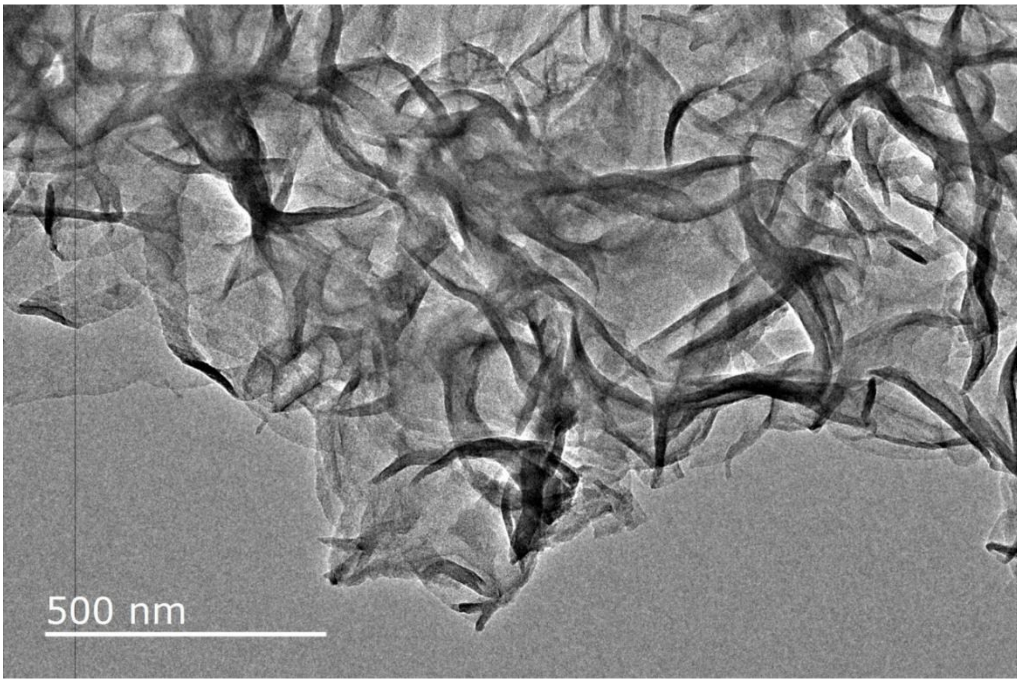

Figure S2. TEM image of CsCNBs-0.

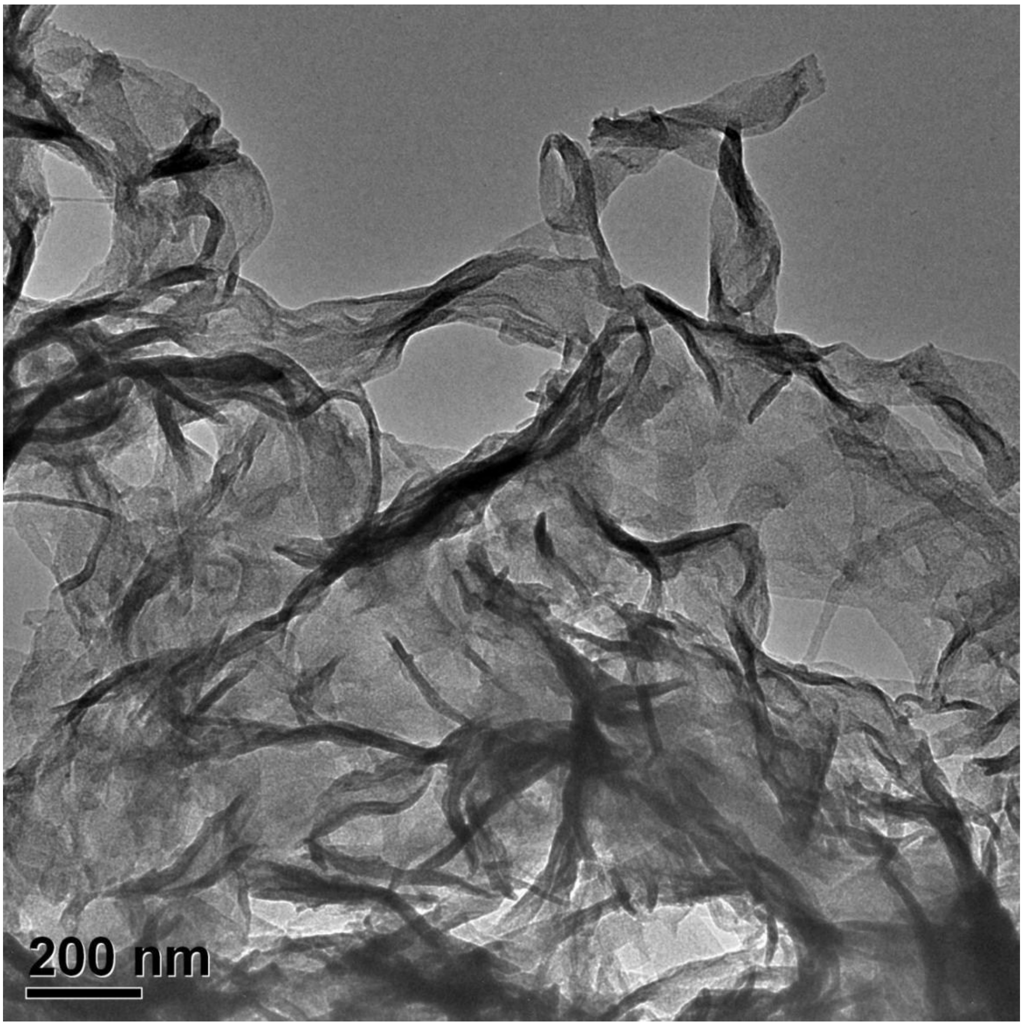

Figure S3. TEM image of CsCNBs heated at 1600 °C.

Table S2. The elemental components of CsPNBs and CsCNBs.

| | N (%) | C (%) | H (%) | S (%) | O (%) [a] |
|---|---|---|---|---|---|
| CsPNBs | 0.09 | 67.02 | 3.688 | 0.226 | 28.976 |
| CsCNBs-0 | 0.8 | 92.33 | 0.222 | 0.956 | 5.692 |
| CsCNBs-20 | 1.06 | 92.12 | 0.91 | 0.69 | 5.22 |
| CsCNBs-40 | 0.77 | 91.86 | 0.746 | 0.923 | 5.701 |
| CsCNBs-60 | 0.72 | 93.25 | 0.681 | 0.819 | 4.53 |

[a] the oxygen contents were figured out by subtracting other components from 100%.

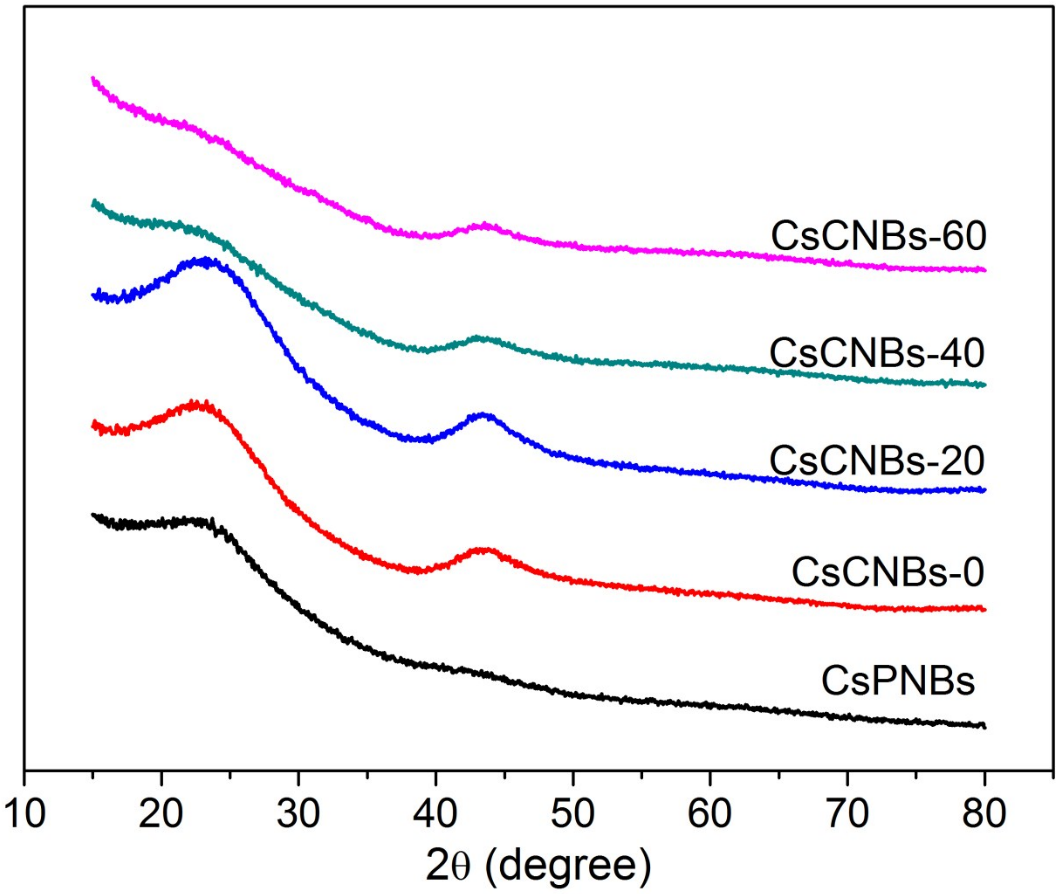


Figure S4. XRD patterns of CsPNBs and CsCNBs.

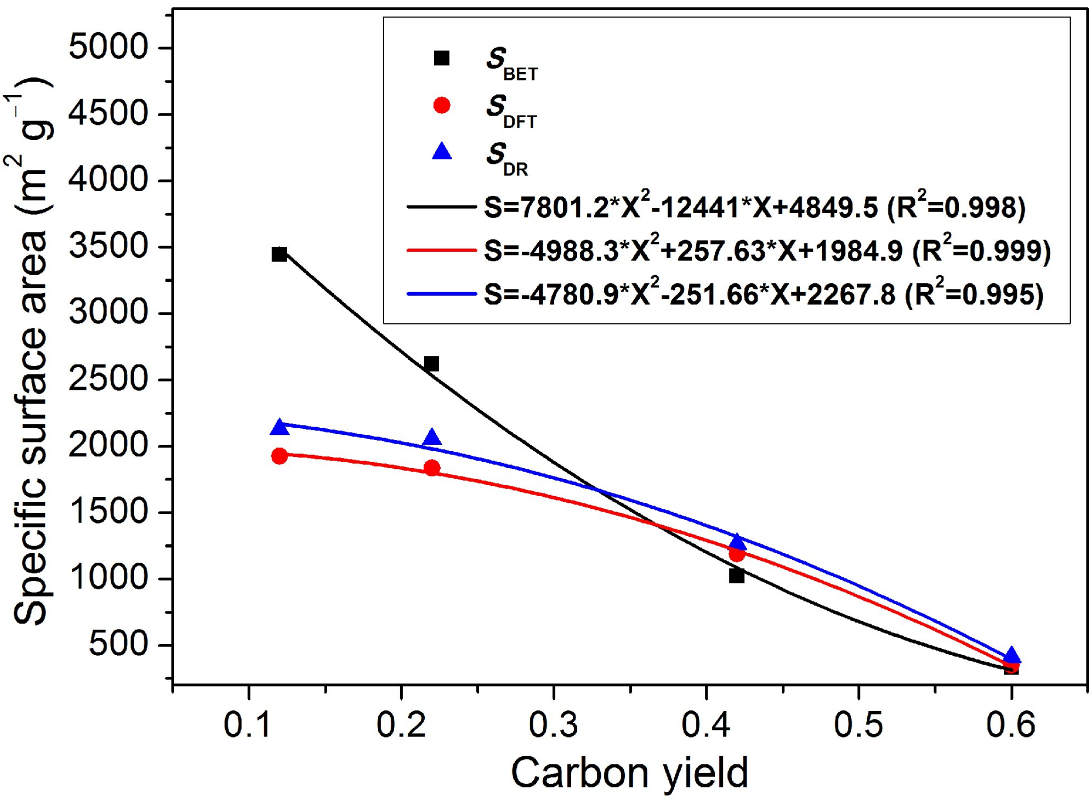


Figure S5 The quadratic relations of $S_{BET}$, $S_{DFT}$ and $S_{DR}$ with carbon yields.

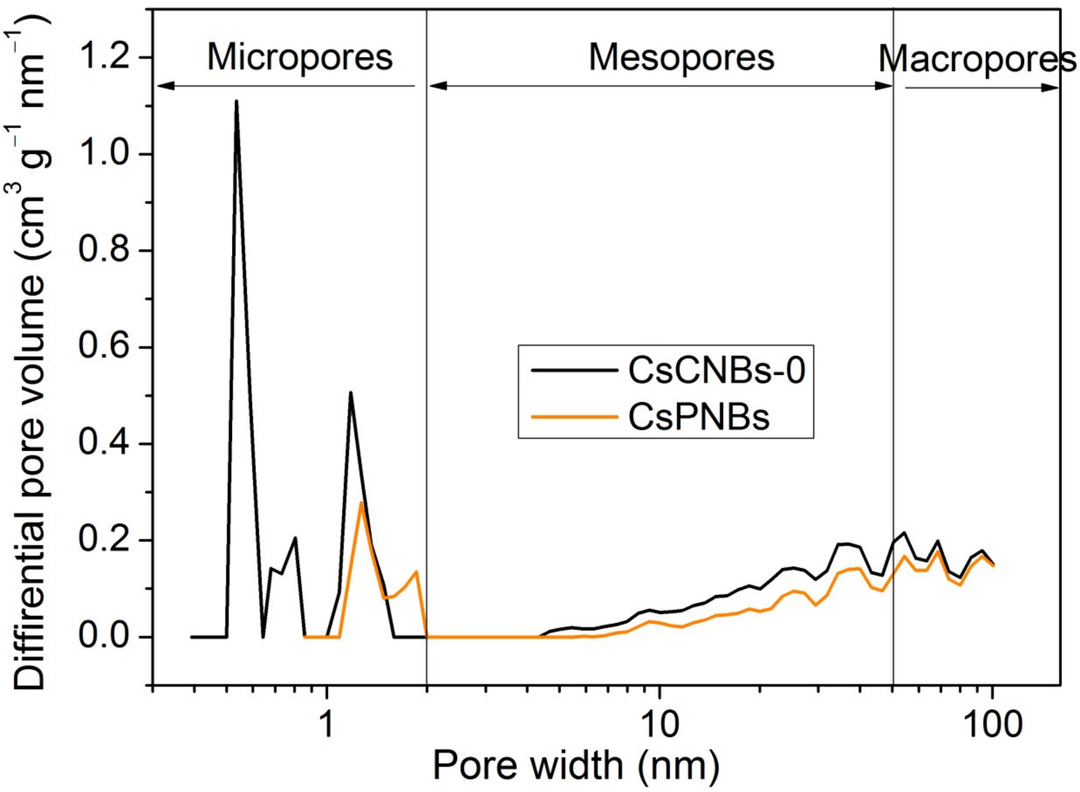


Figure S6. PSD curves of CsPNBs and CsCNBs-0.

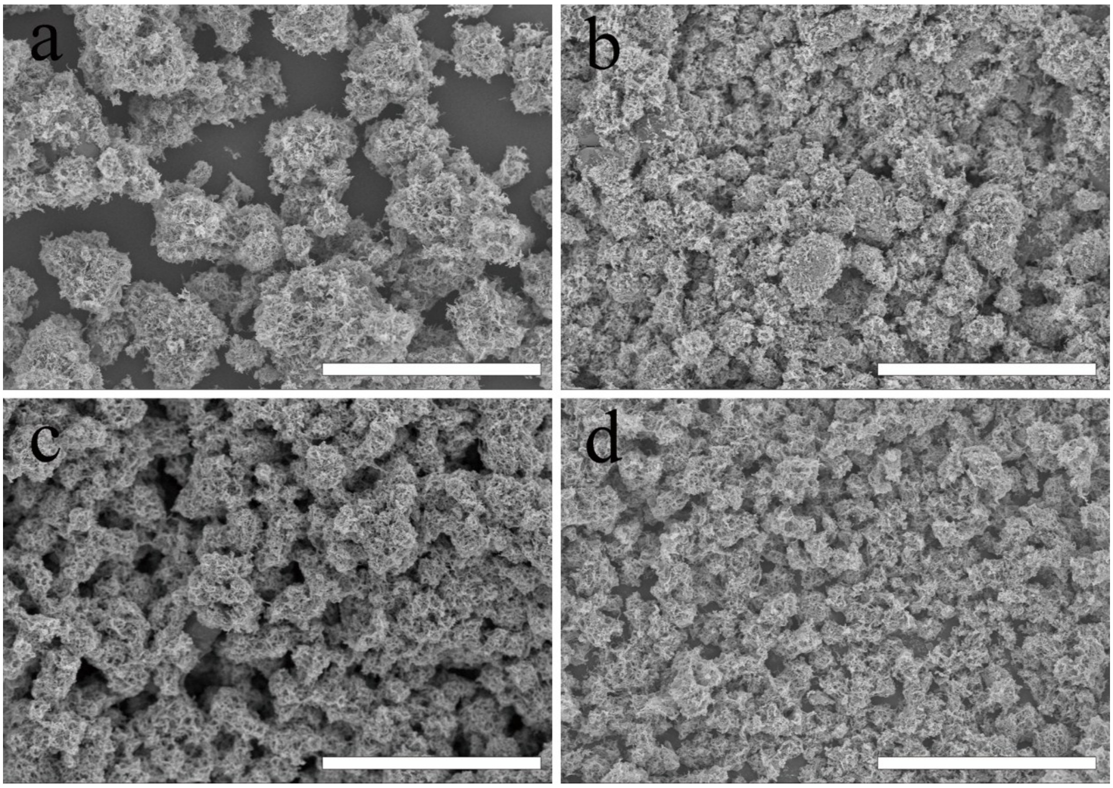


Figure S7. SEM image of a) CsCNBs-0/S, b) CsCNBs-20/S, c) CsCNBs-40/S and d) CsCNBs-60/S. The scale bars are 50 μm.

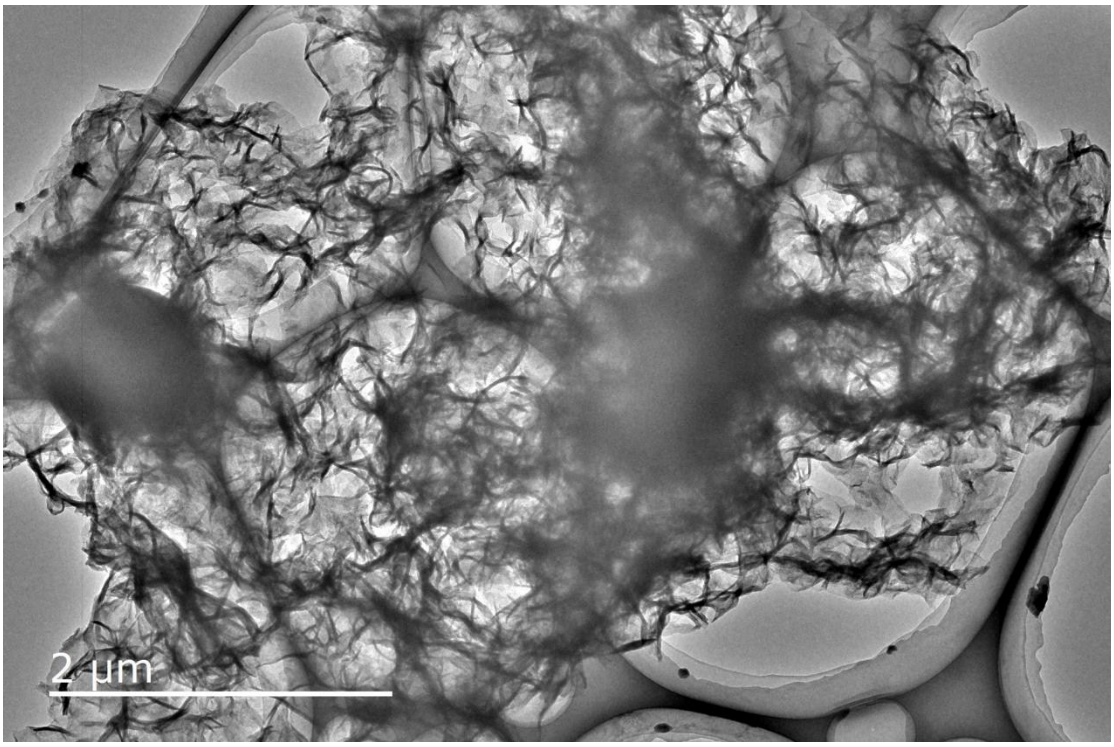


Figure S8. TEM image of CsCNBs-40/S.

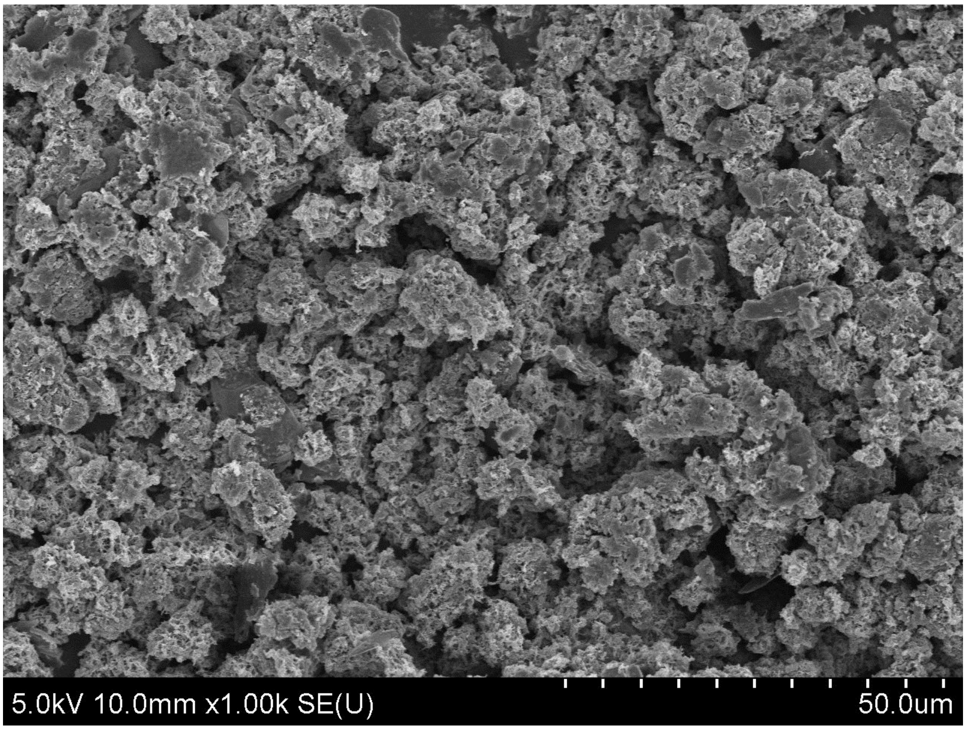


Figure S9 The SEM image of CsCNBs-60/S90.

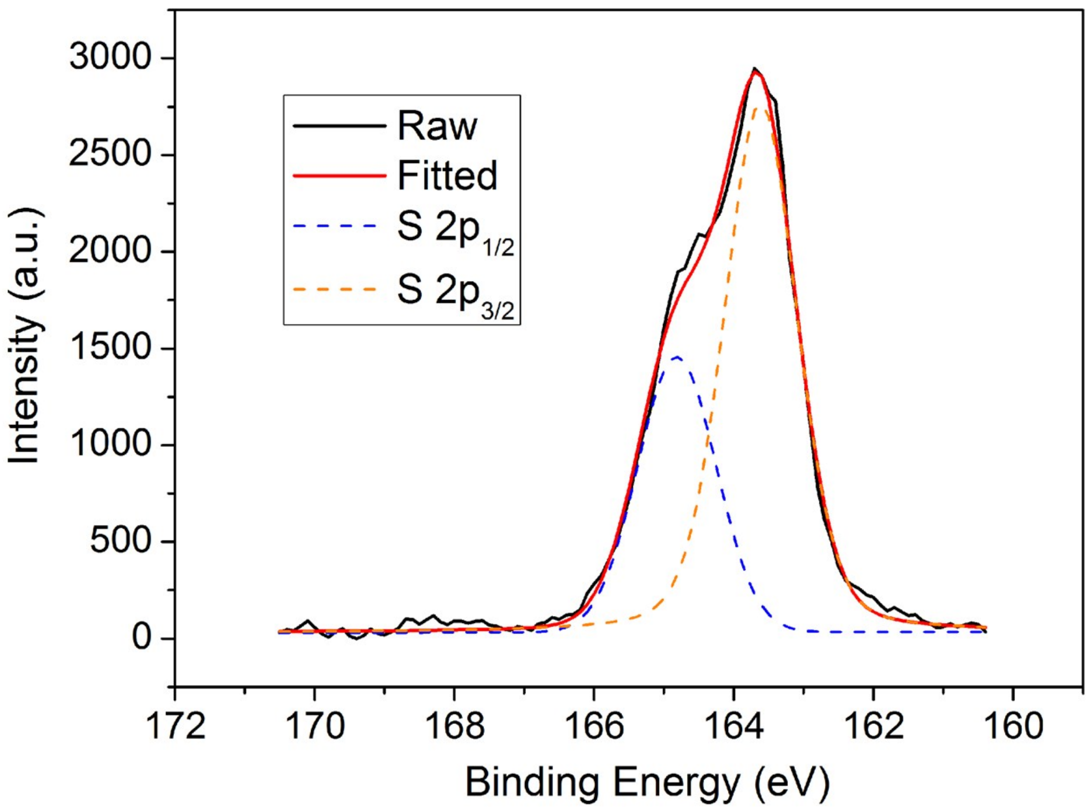


Figure S10. S 2p XPS spectra of CsCNBs-40/S.

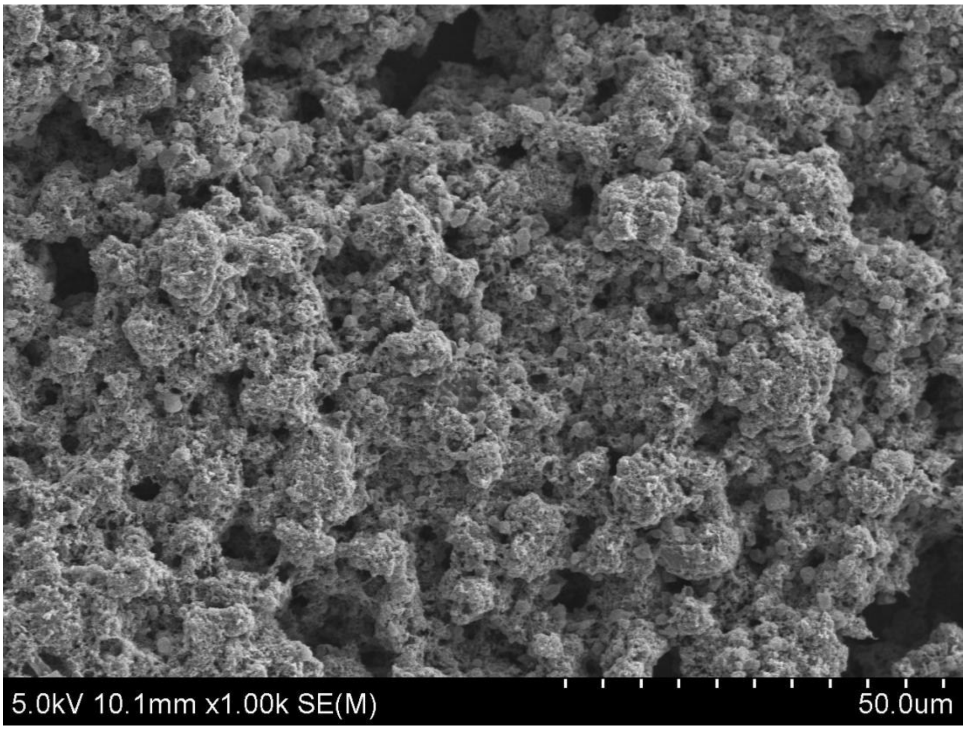


Figure S11. The SEM image of the electrode of CsCNBs-60/S90 after 300 cycles at 1 C.

Table S3. High rate capabilities of some typical carbon-sulfur composites.

| Number | Capacities at 5C (mAh $g^{-1}$) | Capacities at maximum rate (mAh $g^{-1}$) | Voltage window (V) | Sulfur loading | Methods for preparing carbon carriers | References |
|---|---|---|---|---|---|---|
| 1 | / | 738 at 2 C | 1.7 ~ 2.8 | 68.3% | Agar, KOH as activator and template | [3] |
| 2 | 1200 | 453 at 40 C | 1.0 ~ 3.0 | 80.8% | AAO as a template, CVD, Pt end-blocking | [10] |
| 3 | / | 815 at 2 C | 1.8 ~ 2.8 | 50% | Graphene nanosheets, hydrothermal | [11] |
| 4 | 980 | 658 at 20 C | 1.5 ~ 3.0 | 45.2% | CNTs, KOH activation, $ZrO_2$ incorporation | [12] |
| 5 | 861 | 663 at 10 C | 1.7 ~ 2.6 | 71.5% | Hyperbranched MgO | [13] |

| | | | | | | |
|---|---|---|---|---|---|---|
| | | | | | nanowires as templates, CVD | |
| 6 | 728 | 728 at 5 C | 1.7 ~ 2.8 | 68.9% | MWCNTs, KOH activation, graphene coating | [14] |
| 7 | 960 | 879 at 10 C | 1.9 ~ 2.6 | 50% | superaligned CNTs | [15] |
| 8 | / | 800 at 6 C | 1.5 ~ 2.8 | 40% | cetyltrimethyl ammonium bromide (CTAB)-modified sulfur-graphene oxide composite | [16] |
| 9 | 954 | 954 at 5 C | 1.5 ~ 3.0 | 85.2% | AAO as a template, CVD | [17] |
| 10 | / | 1089 at 4 C | 1.0 ~ 2.8 | 70% | Monodispersed sulfur nanoparticles supported on GO | [18] |
| 11 | 1034 | 734 at 10 C | 1.7 ~ 2.8 | 64% | mesoporous metal oxide flakes as templates, CVD | [19] |
| 12 | / | 410 at 8 C | 1.2 ~ 2.8 | 66% | Electrical field induced deposition, vertically aligned sulfur-graphene nanowalls on substrates | [20] |
| 13 | 500 | 500 at 5 C | 1.5 ~ 3.0 | 90% | NaCl and $Na_2S$ as templates, | [21] |

| | | | | | | |
|---|---|---|---|---|---|---|
| | | | | | freeze-dry | |
| 14 | 541 | 541 at 5 C | 1.7 ~ 2.6 | 86% | 1,3,5-trimethylbenzene, silica and Pluronic F127 as co-templates | [22] |
| 15 | 606 | 606 at 5 C | 1.7 ~ 2.8 | 65.2% | Nitrogen-doped graphene | [23] |
| 16 | 880 | 810 at 10 C | 1.5 ~ 3.0 | 50% | 2D layered double oxide as catalyst and template, CVD, KOH activation | [24] |
| 17 | 885 | 885 at 5 C | 1.7 ~ 3.0 | 60% | Direct carbonization and $CO_2$ activation | This work |

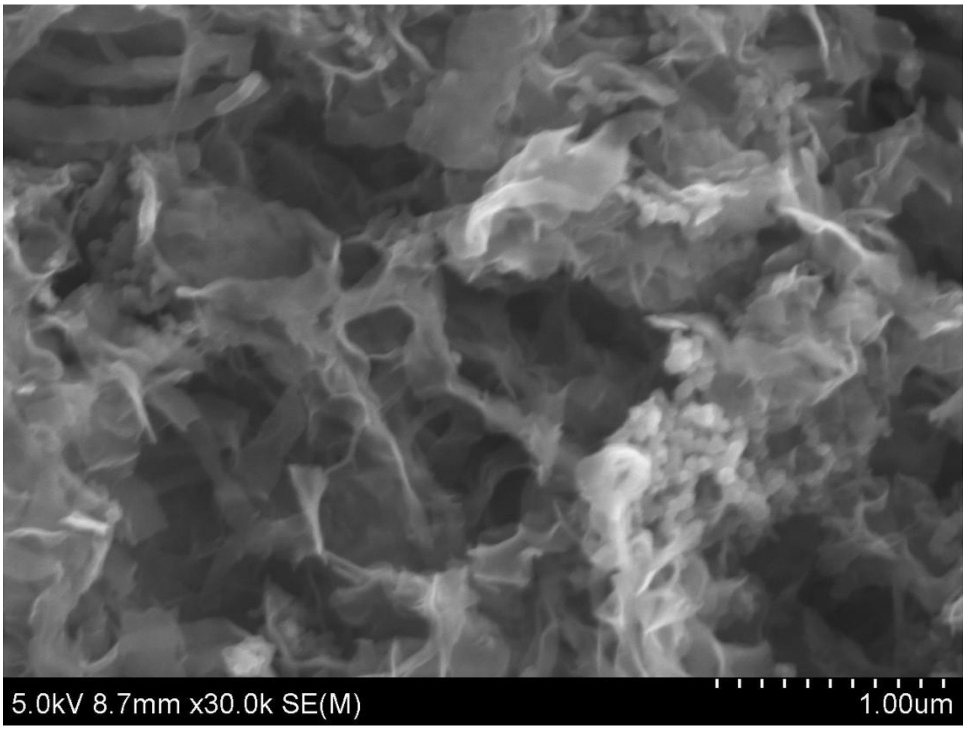


Figure S12. Enlarged SEM image of the electrode of CsCNBs-40/S after 300 cycles at 1 C.

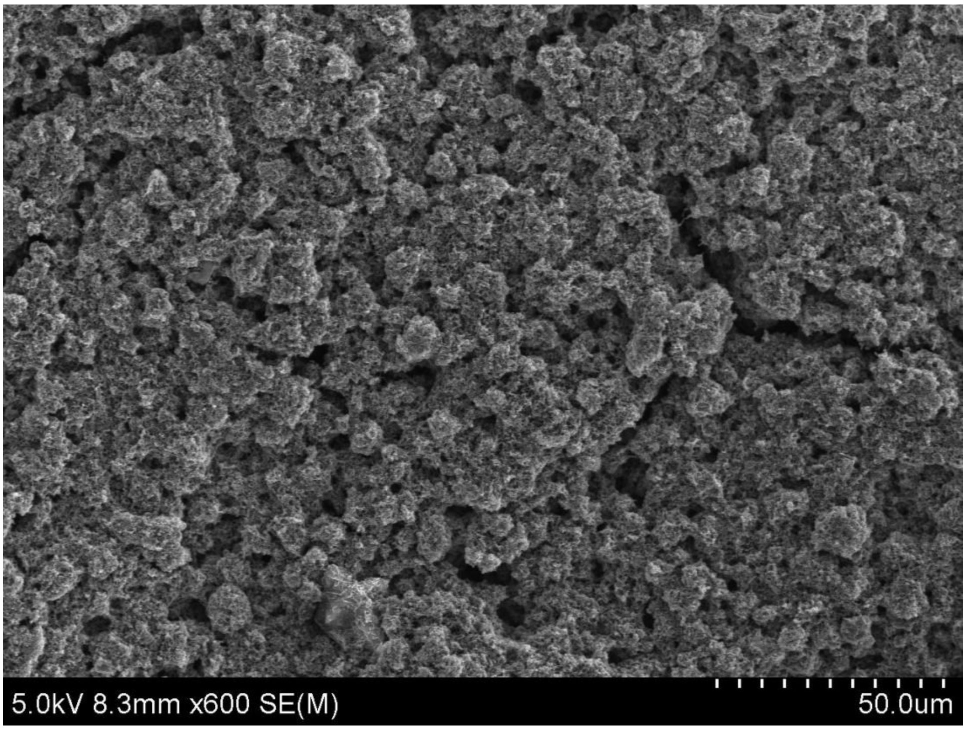


Figure S13. SEM image of the electrode of CsCNBs-40/S after 300 cycles at 1 C.

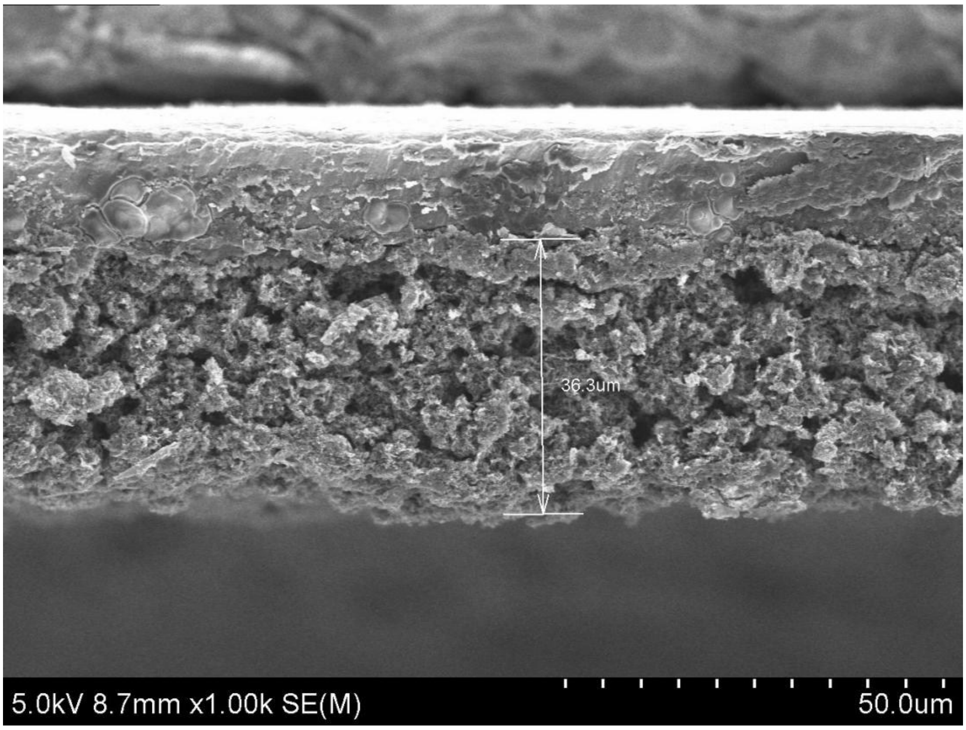


Figure S14. SEM image of the cross section of CsCNBs-40/S after 300 cycles at 1 C.

## References


[1] S. Wei, H. Zhang, Y. Huang, W. Wang, Y. Xia, Z. Yu, Energy Environ. Sci. 4 (2011) 736-740.
[2] G. He, X. Ji, L. Nazar, Energy Environ. Sci. 4 (2011) 2878-2883.
[3] S. Rehman, X. Gu, K. Khan, N. Mahmood, W. Yang, X. Huang, S. Guo, Y. Hou, Adv. Energy Mater. 6 (2016) 1502518.
[4] J. Hou, C. Cao, F. Idrees, X. Ma, Acs Nano, 9 (2015) 2556-2564.
[5] L. Qie, W. Chen, H. Xu, X. Xiong, Y. Jiang, F. Zou, X. Hu, Y. Xin, Z. Zhang, Y. Huang, Energy Environ. Sci. 6 (2013) 2497-2504.
[6] Z. Lyu, D. Xu, L. Yang, R. Che, R. Feng, J. Zhao, Y. Li, Q. Wu, X. Wang, Z. Hu, Nano Energy 12 (2015) 657-665.
[7] C. Hoffmann, S. Thieme, J. Brückner, M. Oschatz, T. Biemelt, G. Mondin, H. Althues, S. Kaskel, ACS Nano 8 (2014) 12130-12140.
[8] P. Strubel, S. Thieme, T. Biemelt, A. Helmer, M. Oschatz, J. Brückner, H. Althues, S. Kaskel, Adv. Funct. Mate. 25 (2015) 287-297.
[9] K. Xia, Q. Gao, J. Jiang, J. Hu, Carbon 46 (2008) 1718-1726.
[10] S. Moon, Y.H. Jung, W.K. Jung, D.S. Jung, J.W. Choi, D.K. Kim, Adv. Mater. 25 (2013) 6547-6553.
[11] C. Zu, A. Manthiram, Advanced Energy Materials, 3 (2013) 1008-1012.
[12] Y. Zhou, C.G. Zhou, Q.Y. Li, C.J. Yan, B. Han, K.S. Xia, Q. Gao, J.P. Wu, Adv. Mater. 27 (2015) 3774-3781.
[13] S. Chen, X. Huang, H. Liu, B. Sun, W. Yeoh, K. Li, J. Zhang, G. Wang, Adv. Energy Mater. 4 (2014) 1301761.
[14] J. Xie, J. Yang, X. Zhou, Y. Zou, J. Tang, S. Wang, F. Chen, J. Power Sources 253 (2014) 55-63.
[15] L. Sun, M. Li, Y. Jiang, W. Kong, K. Jiang, J. Wang, S. Fan, Nano lett. 14 (2014) 4044-4049.
[16] M.-K. Song, Y. Zhang, E.J. Cairns, Nano lett. 13 (2013) 5891-5899.
[17] F. Jin, S. Xiao, L. Lu, Y. Wang, Nano lett. 16 (2016) 440-447.
[18] H.W. Chen, C.H. Wang, W.L. Dong, W. Lu, Z.L. Du, L.W. Chen, Nano lett. 15 (2015) 798-802.
[19] M.-Q. Zhao, Q. Zhang, J.-Q. Huang, G.-L. Tian, J.-Q. Nie, H.-J. Peng, F. Wei, Nat. Commun. 5 (2014).
[20] B. Li, S. Li, J. Liu, B. Wang, S. Yang, Nano lett. 15 (2015) 3073-3079.
[21] G. Li, J. Sun, W. Hou, S. Jiang, Y. Huang, J. Geng, Nat. Commun. 7 (2016) 10601.
[22] S. Chen, X. Huang, B. Sun, J. Zhang, H. Liu, G. Wang, J. Mater. Chem. A, 2 (2014) 16199-16207.
[23] Y. Qiu, W. Li, W. Zhao, G. Li, Y. Hou, M. Liu, L. Zhou, F. Ye, H. Li, Z. Wei, S. Yang, W. Duan, Y. Ye, J. Guo, Y. Zhang, Nano lett. 14 (2014) 4821-4827.
[24] H.-J. Peng, J.-Q. Huang, M.-Q. Zhao, Q. Zhang, X.-B. Cheng, X.-Y. Liu, W.-Z. Qian, F. Wei, Adv. Funct. Mater. 24 (2014) 2772-2781.